NASA Technical Paper 3024

September 1990

# Buckling and Postbuckling Behavior of Compression-Loaded Isotropic Plates With Cutouts

Michael P. Nemeth



**NASA Technical Paper 3024**

1990

# Buckling and Postbuckling Behavior of Compression-Loaded Isotropic Plates With Cutouts

Michael P. Nemeth
*Langley Research Center*
*Hampton, Virginia*

National Aeronautics and Space Administration
Office of Management
Scientific and Technical Information Division

## Summary

An experimental study of the buckling and postbuckling behavior of square and rectangular compression-loaded aluminum plates with centrally located circular, square, and elliptical cutouts is presented. Experimental results indicate that the plates exhibit overall trends of increasing buckling strain and decreasing initial postbuckling stiffness with increasing cutout width. Corresponding plates with circular and square cutouts of the same width buckle at approximately the same strain level and exhibit approximately the same initial postbuckling stiffness. Results show that the reduction in initial postbuckling stiffness due to a cutout generally decreases as the plate aspect ratio increases. Other results presented in this paper indicate that square plates with elliptical cutouts and a large ratio of cutout width to plate width generally lose prebuckling and initial postbuckling stiffness as the cutout height increases. However, the plates buckle at essentially the same strain level. Results also indicate that postbuckling stiffness is more sensitive to changes in elliptical cutout height than are prebuckling stiffness and buckling strain.

## Introduction

An important structural component used in practically all aerospace vehicles is the rectangular plate with a centrally located cutout. Cutouts commonly appear in plates as access ports for mechanical and electrical systems or are included to reduce the structural weight in components such as wing ribs and spars. Often during vehicle operation, these members experience compression loads, and thus their buckling and postbuckling behavior are important factors that must be considered in their design.

Investigations of the buckling behavior of plates with cutouts have appeared in the technical literature since 1943. A summary of these investigations, for both isotropic and laminated composite plates, is given in reference 1. In-depth parametric studies of the buckling behavior of square and rectangular plates with central circular cutouts are presented in references 1 through 3. Analytical and experimental results are presented in these studies that indicate buckling behavior trends for a wide range of plate parameters. The results and physical insight presented in these references indicate that the buckling behavior of compression-loaded isotropic and orthotropic plates with cutouts is well understood.

Substantially fewer studies of the postbuckling behavior of plates with cutouts are available in the technical literature. Some of the first studies are presented in references 4 through 7. The results presented in references 4 and 6 address the postbuckling collapse of steel beams, columns, and plate girder structures with cutouts in their webs. The results presented in references 5 and 7 focus specifically on square and rectangular isotropic plates with central circular cutouts. Buckling and postbuckling results are also presented in reference 5 for square laminated composite plates with central circular cutouts.

More recently, selected results for the postbuckling and failure characteristics of compression-loaded rectangular graphite-epoxy plates with central circular cutouts have been presented in reference 8. Additional recent studies of the postbuckling collapse of square isotropic plates with square and circular cutouts are presented in references 9 and 10. A study of the imperfection sensitivity and postbuckling strength of compression-loaded square isotropic and laminated composite plates with central circular cutouts is presented in reference 11.

An experimental study of the postbuckling behavior of square compression-loaded graphite-epoxy and aluminum plates with central circular cutouts is presented in reference 12. This study indicates the overall postbuckling behavior trends of the plates as a function of plate orthotropy and cutout size.

Review of the studies presented in references 4 through 12 indicates that the effects of cutout size, plate aspect ratio, cutout shape, and laminate stacking sequence on the postbuckling behavior of plates are still not well understood. This paper examines the behavior of selected isotropic compression-loaded square and rectangular plates and attempts to establish overall trends indicating some of the effects of cutout size, cutout shape, and plate aspect ratio on plate postbuckling behavior. The paper focuses on an experimental study of rectangular aluminum plates with centrally located circular, square, and elliptical cutouts.

The author wishes to acknowledge Philip D. Sydow for his help in conducting several of the laboratory experiments and for providing some computer assistance.

## Symbols

| | |
|---|---|
| $a$ | half-height of elliptical cutout (see fig. 10), cm (in.) |
| $b$ | half-width of elliptical cutout (see fig. 10), cm (in.) |
| $d$ | cutout diameter (see fig. 1(b)), cm (in.) |
| EA | prebuckling stiffness of a plate, N (lb) |
| $L$ | plate length (see fig. 1(b)), cm (in.) |
| $L_b$ | plate length between ends of test fixture (see fig. 1(b)), cm (in.) |

$P$ axial load (see fig. 2), N (lb)

$P_{cr}$ axial load at buckling (see fig. 3), N (lb)

$P_{cr}^{o}$ analytically obtained axial load at buckling for plates without cutouts (see fig. 4), N (lb)

$s$ height and width of a square cutout (see fig. 5), cm (in.)

$t$ plate thickness, cm (in.)

$W$ plate width (see fig. 1(b)), cm (in.)

$W_h$ plate width between sides of test fixture (see fig. 1(b)), cm (in.)

$\Delta$ end-shortening (see fig. 2), cm (in.)

$\Delta_{cr}^{o}$ analytically obtained end-shortening at buckling for plates without cutouts (see fig. 2), cm (in.)

## Specimens, Apparatus, and Tests

The specimens tested in this investigation were machined out of 6061-T6 aluminum sheets with a nominal thickness of 1.59 mm (0.0625 in.). Specimens were machined into rectangular plates with plate aspect ratios $L/W$ of 1, 3, and 5, where $L$ is the plate length and $W$ is the plate width. The square plates had a nominal length and width of 25.40 cm (10.00 in.). The rectangular plates with $L/W = 3$ and 5 had a nominal width of 10.160 cm (4.00 in.) and nominal lengths of 30.480 cm and 50.800 cm (12.00 in. and 20.00 in.), respectively. The loaded edges of each specimen were machined flat and parallel to permit uniform compressive loading. Nominal material properties of each plate were assumed to include a Young's modulus $E$ of 76.0 GPa ($11.0 \times 10^6$ psi) and a Poisson's ratio $\nu$ of 0.33.

Central circular cutouts were machined into six of the square panels with a milling machine. The circular cutout diameters ranged from 2.413 cm (0.95 in.) to 14.478 cm (5.70 in.). Central circular and square cutouts were also machined into 16 of the rectangular panels. The circular cutout diameters in the rectangular panels ranged from 1.270 cm (0.50 in.) to 7.620 cm (3.00 in.). For each panel with a circular cutout, a panel was machined for a square cutout with a cutout length and width equal to the corresponding circular cutout diameter. The square cutouts had reentrant corners with a corner radius of 1.59 mm (0.0625 in.). Several thickness measurements were made on each square and rectangular specimen, and the average thickness for both groups was 1.64 mm (0.0647 in.). Similarly, central elliptical cutouts were machined into seven of the square panels with a six-axis numerically controlled milling machine. The widths of the elliptical cutouts (in the same direction as the plate width) were kept at a constant value of 14.480 cm (5.70 in.), and the cutout heights ranged from 1.207 cm (0.475 in.) to 16.891 cm (6.65 in.). Several thickness measurements were made on each square specimen with an elliptical cutout, and the average thickness was 1.59 mm (0.0625 in.). A total of 34 specimens were tested. The specimen designations and cutout dimensions are given in tables 1 through 6.

The specimens were loaded gradually in axial compression with a 0.53-MN-capacity (120-kip) hydraulic testing machine. The loaded ends of the specimens were clamped by fixtures during testing, and the unloaded edges were simply supported by restraints that prevent the specimen from buckling as a wide column. The specimens were loaded to approximately twice the buckling load, and then the test was stopped. One side of each specimen was painted white to reflect light so that a moire-fringe technique could be used to monitor the out-of-plane deformations. A typical specimen mounted in the test fixture is shown in figure 1(a).

Electrical resistance strain gages were used to measure strains, and direct-current differential transformers were used to measure axial displacements and displacements normal to the specimen surface. Electrical signals from the instrumentation and the corresponding applied loads were recorded on magnetic tape at regular time intervals during the tests.

## Results and Discussion

Results are presented for aluminum plates with several different plate aspect ratios, cutout sizes, and cutout shapes. First, the procedures used to obtain the experimental values of the prebuckling stiffnesses, buckling loads, and initial postbuckling stiffnesses are presented. Results are then presented in separate subsections for the square plates with circular cutouts, the rectangular plates with circular and square cutouts, and the square plates with elliptical cutouts. After these subsections, results indicating the overall behavior trends exhibited by the specimens are presented.

### Interpretation of Test Data

To illustrate the postbuckling behavior of plates with cutouts, curves of nondimensional load versus end-shortening are presented in this paper. The curve of nondimensional load versus end-shortening for each specimen was obtained by first performing a least-squares fit of a straight line to the most linear part of the primary branch of the plot of actual load versus end-shortening recorded during the

test. With the equation of the line obtained from the least-squares fit of the test data, the prebuckling stiffness was obtained directly, and the initial irregularity in the plot of actual load versus end-shortening, associated with initial slack in the test fixture, was eliminated. Similarly, the initial postbuckling stiffness was obtained directly by performing a least-squares fit of a straight line to the most linear part of the secondary branch of the plot of load versus end-shortening recorded during testing. The experimental buckling load and associated end-shortening were then obtained by computing the intersection of the two straight lines fitted to the primary and secondary branches of the test data for load versus end-shortening.

Finally, the curves were nondimensionalized by dividing the load and end-shortening of a given specimen by approximate analytical values of the buckling load $P^o_{cr}$ and end-shortening $\Delta^o_{cr}$, respectively, of the corresponding plate without a cutout. These approximate analytical values were obtained from solutions of the standard boundary-value problem of a rectangular region with boundary conditions specified on the edges. The values are referred to herein as approximate, since this standard boundary-value problem does not exactly represent the boundary-value problem of the experiments. In the experiments, the prebuckling stiffness, deformations, and stresses in the plate are influenced by the true length $L$ and width $W$ of a given specimen. However, when the plate buckles, the unsupported length $L_b$ and unsupported width $W_b$, shown in figure 1(b), strongly influence the buckling response. The approximate analytical values obtained from the standard boundary-value problem were based on the nominal material properties given previously and on a plate thickness of 0.1643 cm (0.0647 in.). Moreover, the analytical values were based on a uniaxial loading condition in which two opposite edges of the plate are uniformly displaced toward one another. The loaded edges were assumed to be clamped, and the unloaded edges were assumed to be simply supported. In the calculations of $P^o_{cr}$ and $\Delta^o_{cr}$ for the square plates, the buckling load and corresponding end-shortening were based on the 24.130-cm (9.50-in.) unsupported width $W_b$ between knife-edge supports of the test fixture. For the 30.480-cm long (12.00-in.) and 50.800-cm long (20.00-in.) rectangular plates, buckling stress resultants were computed based on $W_b = 8.890$ cm (3.50 in.). The buckling loads were obtained by multiplying the buckling stress resultants by the true 10.160-cm (4.00-in.) width of the plates. The true width was used to compute the buckling load because of the relatively small values of $W_b/W$ and $L_b/L$ for the rectangular plates compared with those of the square plates. Similarly, the critical end-shortenings of the rectangular plates are also based on the true 10.160-cm (4.00-in.) width of the true lengths of the plates.

The experimental results for the plates with very large ratios of cutout width to plate width exhibited nonlinear prebuckling deformations. This attribute made it difficult to establish the experimental buckling load in the manner previously described. For these cases, the experimental buckling load was estimated from the data for load versus transverse deflection and from strain-gage data. The initial postbuckling stiffness was taken to be the slope of a line tangent to the secondary branch of the plot of load versus end-shortening at the estimated buckling load. For these cases, the value of the initial postbuckling stiffness is sensitive to the estimate of the buckling load.

### Square Plates With Circular Cutouts

Experimental results were obtained for a square plate without a cutout and for square plates with six different cutout sizes. Each plate has a ratio of plate width to plate thickness $W/t$ of approximately 155. The cutout size, buckling load, prebuckling stiffness, and postbuckling stiffness of each plate are presented in table 1. Curves of nondimensional load $P/P^o_{cr}$ versus nondimensional end-shortening $\Delta/\Delta^o_{cr}$ are presented in figure 2, where $P$ is the axial load, $\Delta$ is the end-shortening, and $P^o_{cr}$ and $\Delta^o_{cr}$ are the analytically obtained buckling load and associated end-shortening of the corresponding plate without a cutout, respectively. Buckling is indicated by the filled circles in the figure. Results are presented in this figure for ratios of cutout diameter to plate width $d/W_b$ from 0 to 0.6.

The results presented in table 1 and figure 2 indicate that the prebuckling stiffnesses of the plates decrease monotonically with increasing cutout size. This trend is consistent with the fact that an increase in cutout size gives rise to a decrease in the cross-sectional area at the net section of the plate. The maximum decrease in prebuckling stiffness compared with the stiffness of the plate without a cutout is approximately 42 percent for the plate with $d/W_b = 0.6$.

The results in table 1 also indicate that the buckling loads of the plates decrease at first and then tend to increase with increasing cutout size. Analytical results indicating a similar trend for the buckling loads are presented in references 1 and 7. Average buckling strains obtained analytically with the computer program described in reference 13 and the average buckling strains of the test specimens are shown in figure 3. The average buckling strains

shown in this figure are defined by the ratio of buckling load to prebuckling stiffness $P_{cr}/EA$, and are plotted as a function of the ratio of cutout diameter to plate width $d/W_b$. Similar results are shown in figure 3 for plates with square cutouts as a function of the ratio of square-cutout width to plate width $s/W_b$. These results indicate a similar trend of increasing buckling strain with increasing cutout size, and suggest that the increase in experimental buckling strain with increasing cutout size presented herein is not due entirely to scatter in the test data. The buckling mode shapes for all the plates, except the one with $d/W_b = 0.5$, consisted of one half-wave along both the length and width. The plate with $d/W_b = 0.5$ buckled into a mode that was somewhat off-centered compared with the buckle patterns of the other plates.

Additional results presented in table 1 and figure 2 indicate that the initial postbuckling stiffnesses of the plates decrease monotonically with increasing cutout size. The largest decrease is approximately 43 percent for $d/W_b = 0.6$. Comparing the prebuckling stiffness with the postbuckling stiffness given in table 1 for each specimen indicates that, as the cutout size increases, the reduction in axial stiffness due to buckling varies between 35 and 40 percent for the full range of cutout sizes.

### Rectangular Plates With Circular and Square Cutouts

Experimental results were obtained for two rectangular plates without a cutout and with plate aspect ratios $L/W$ of 3, and for two plates without a cutout and with $L/W = 5$. Results were also obtained for similar rectangular plates ($L/W = 3$ and 5) with four different circular cutout sizes and four different square-cutout sizes. Specifically, for each plate with a given $L/W$ and circular cutout of diameter $d$, there is a corresponding plate with a square cutout and a height and width $s$ equal to $d$. Each plate has a ratio of plate width to plate thickness $W/t$ of approximately 62. The cutout size, buckling load, prebuckling stiffness, and postbuckling stiffness of each plate with $L/W = 3$ and with a circular cutout and each plate with $L/W = 3$ and with a square cutout are presented in tables 2 and 3, respectively. Similarly, the cutout size, buckling load, prebuckling stiffness, and postbuckling stiffness of each plate with $L/W = 5$ and with a circular cutout and each plate with $L/W = 5$ and with a square cutout are presented in tables 4 and 5, respectively. Curves of nondimensional load $P/P^o_{cr}$ versus nondimensional end-shortening $\Delta/\Delta^o_{cr}$ are presented in figures 4 and 5 for the plates with circular and square cutouts and with $L/W = 3$, respectively, and are presented in figures 6 and 7 for the plates with circular and square cutouts and with $L/W = 5$, respectively. Buckling is indicated by the filled circles on the figures. The results shown in figures 4 and 6 for the plates with circular cutouts are presented as a function of the ratio of cutout diameter to plate width $d/W_b$. Similarly, the results shown in figures 5 and 7 for the plates with square cutouts are presented as a function of the ratio of cutout width to plate width $s/W_b$.

***Plates with $L/W = 3$ and with circular cutouts.*** The results presented in table 2 and figure 4 indicate that the prebuckling stiffnesses of the plates with $L/W = 3$ and with circular cutouts generally decrease with increasing cutout size. The maximum decrease in prebuckling stiffness compared with the average stiffnesses of the two plates without a cutout is approximately 47 percent for the plate with $d/W_b = 0.86$. The plate with $d/W_b = 0.57$ exhibited approximately 20 percent less prebuckling stiffness than the two plates without a cutout.

The results in table 2 and figure 4 also indicate that the buckling loads of the plates decrease at first and then tend to increase with increasing cutout size in a manner similar to that exhibited by the square plates. The buckling loads given in table 2 for the plate with $d/W_b = 0.86$ were estimated from the data that show the load versus out-of-plane deflection at various points on the plate and from the strain-gage data shown in figure 8. The results presented in figure 8 show the axial strain as a function of the nondimensional loading $P/P^o_{cr}$ obtained from back-to-back strain gages mounted adjacent to the edge of the cutout. Average buckling strains obtained analytically with the computer program described in reference 13 and the average buckling strains of the test specimens are also shown in figure 3. These analytically obtained buckling-strain trends and the closeness of the results for the two plates tested without cutouts (fig. 3) suggest that an increase in experimental buckling strain with increasing cutout size is not a manifestation of scatter in the test data. The buckling mode shapes for all the plates with $L/W = 3$ and with $d/W_b \leq 0.57$ consisted of three half-waves along the length and one half-wave along the width. The strain-gage data shown in figure 8 and other experimental data indicate that the plate with $d/W_b = 0.86$ buckled locally around the cutout. The plate first buckled inelastically into a mode shape with one axial half-wave along the shaded region shown on the sketch in figure 8; it then changed to a mode shape that consisted of two axial half-waves. Both local mode shapes had very small amplitudes compared with the amplitudes of

the global mode shapes of the other plates and could not be detected by the moire-fringe technique.

Results presented in table 2 and figure 4 also indicate that the initial postbuckling stiffnesses of the plates generally decrease with increasing cutout size. The largest decrease is approximately 78 percent for $d/W_b = 0.86$. The experimental results indicate that this plate exhibited nonlinear prebuckling deformations as a result of the yielding of the material near the net section of the plate. The actual value of the postbuckling stiffness given in table 2 is the tangent stiffness at the estimated value of the buckling load. The plate with $d/W_b = 0.57$ behaved elastically in the initial part of the postbuckling range and exhibited approximately 19 percent less initial postbuckling stiffness than the two plates without a cutout. Comparing the prebuckling stiffness with the postbuckling stiffness given in table 2 for each specimen indicates that, as the cutout size increases up to $d/W_b = 0.57$, the reduction in axial stiffness due to buckling varies between 40 and 31 percent. For the plate with $d/W_b = 0.86$, the reduction in axial stiffness is approximately 82 percent.

***Plates with $L/W = 3$ and with square cutouts.*** The results presented in table 3 and figure 5 indicate that the prebuckling stiffnesses of the plates with $L/W = 3$ and with square cutouts also generally decrease with increasing cutout size. The maximum decrease in prebuckling stiffness compared with the average stiffnesses of the two plates without a cutout is approximately 55 percent for the plate with $s/W_b = 0.86$. The plate with $s/W_b = 0.57$ exhibited approximately 24 percent less prebuckling stiffness than the two plates without a cutout.

The results presented in table 3 and figure 5 also indicate that the buckling loads of the plates decrease at first and then increase with increasing cutout size. The buckling load given in table 3 for the plate with $s/W_b = 0.86$ was also estimated by using the data that show the load versus out-of-plane deflection at various points on the plate and by using the strain-gage data. Average buckling strains obtained analytically and the average buckling strains of the test specimens are also shown in figure 3. These results show a trend of increasing experimental buckling strain with increasing cutout size. The buckling mode shapes for all the plates with $L/W = 3$ and with $s/W_b \leq 0.29$ consisted of three half-waves along the length and one half-wave along the width. The buckling mode shape for the plate with $s/W_b = 0.57$ consisted of four half-waves along the length and one half-wave along the width. The buckle patterns for the plates with $s/W_b = 0.29$ and 0.57 are shown in figure 9 along with the buckle patterns for the corresponding plates with circular cutouts. The results show that changing the cutout shape from circular to square can lead to a change in buckle pattern in the plates with the larger cutout sizes. Strain-gage data and out-of-plane deflection data indicate that the plate with $s/W_b = 0.86$ buckled inelastically and locally around the cutout into a mode shape with nine half-waves along the slender rectangular ligament of the plate adjacent to the cutout. The permanently set local mode shape also had a very small amplitude compared with the amplitudes of the global mode shapes of the other plates. The local mode could not be detected by the moire-fringe technique.

Other results presented in table 3 and figure 5 indicate that the initial postbuckling stiffnesses of the plates generally decrease with increasing cutout size. The largest decrease in approximately 90 percent for $s/W_b = 0.86$ and includes the effects of material yielding. The plate with $s/W_b = 0.57$ behaved elastically in the initial part of the postbuckling range and exhibited approximately 24 percent less initial postbuckling stiffness than the two plates without a cutout. Comparing the prebuckling stiffness to the postbuckling stiffness given in table 3 for each specimen indicates that, as the cutout size increases up to $s/W_b = 0.57$, the reduction in axial stiffness due to buckling varies between 40 and 36 percent. For the plate with $s/W_b = 0.86$, the reduction in axial stiffness is approximately 86 percent.

***Plates with $L/W = 5$ and with circular cutouts.*** The results presented in table 4 and figure 6 indicate that the prebuckling stiffnesses of the plates with $L/W = 5$ and with circular cutouts generally decrease with increasing cutout size. The maximum decrease in prebuckling stiffness (compared with the average stiffnesses of the two plates without a cutout) is approximately 35 percent for the plate with $d/W_b = 0.86$ prior to yielding. The plate with $d/W_b = 0.57$ exhibited approximately 10 percent less prebuckling stiffness than the corresponding two plates without a cutout.

The results in table 4 and figure 6 also indicate that the buckling loads of the plates decrease at first and then tend to slightly increase with increasing cutout size. Average buckling strains of the test specimens exhibit a trend similar to the trends shown in figure 3 for the plates with $L/W = 1$ and 3. The buckling mode shapes for all the plates with $L/W = 5$ and with $d/W_b \leq 0.57$ consisted of five half-waves along the length and one half-wave along the width. The strain-gage data and the out-of-plane deflection data indicate that the plate with $d/W_b = 0.86$ yielded in the net section of the plate and buckled into a small-amplitude global mode,

unlike the corresponding plate with $L/W = 3$. The buckling mode shape consisted of five half-waves along the length and one half-wave along the width. However, the amplitude of the half-wave in the central region surrounding the cutout, where yielding occurred, exhibited a substantially smaller amplitude than the other half-waves that made up the mode shape.

Results presented in table 4 and figure 6 indicate that the initial postbuckling stiffnesses of the plates again generally decrease with increasing cutout size. The largest decrease is approximately 74 percent for the plate with $d/W_b = 0.86$ and includes the effects of material yielding. The plate with $d/W_b = 0.57$ behaved elastically in the initial part of the postbuckling range and exhibited approximately 5 percent less initial postbuckling stiffness than the two without a cutout. Comparing the prebuckling stiffness with the postbuckling stiffness given in table 4 for each specimen indicates that, as the cutout size increases up to $d/W_b = 0.57$, the reduction in axial stiffness due to buckling varies between 44 and 40 percent. For the plate with $d/W_b = 0.86$, the reduction in axial stiffness is approximately 77 percent.

***Plates with $L/W = 5$ and with square cutouts.*** The results presented in table 5 and figure 7 indicate that the prebuckling stiffnesses of the plates with $L/W = 5$ and with square cutouts generally decrease with increasing cutout size. The maximum decrease in prebuckling stiffness (compared with the average stiffnesses of the two plates without a cutout) is approximately 43 percent for the plate with $s/W_b = 0.86$ prior to yielding. The plate with $s/W_b = 0.57$ exhibited approximately 24 percent less prebuckling stiffness than the two plates without a cutout.

The results in table 5 and figure 7 also indicate that the buckling loads of the plates decrease at first and then increase with increasing cutout size. Average buckling strains of the test specimens exhibit a trend similar to the trends shown in figure 3. The buckling mode shapes for all the plates with $L/W = 5$ and with $s/W_b \leq 0.29$ consisted of five half-waves along the length and one half-wave along the width. The buckling mode shape for the plate with $s/W_b = 0.57$ consisted of six half-waves along the length and one half-wave along the width. The plate with $s/W_b = 0.86$ buckled inelastically and locally around the cutout into a mode shape with six half-waves along the slender rectangular ligament of the plate adjacent to the cutout. However, the waves appeared to be unequally spaced along the length of the ligament. The local mode shape also had a very small amplitude compared with those of the global mode shapes of the other plates, and could not be detected by the moire-fringe technique.

Results presented in table 5 and figure 7 indicate that the initial postbuckling stiffnesses of the plates generally decrease with increasing cutout size. The largest decrease is approximately 66 percent for $s/W_b = 0.86$ and again includes the effects of material yielding. The plate with $s/W_b = 0.57$ behaved elastically in the initial part of the postbuckling range and exhibited approximately 1 percent less initial postbuckling stiffness than the two plates without a cutout. Comparing the prebuckling stiffness with the postbuckling stiffness given in table 5 for each specimen indicates that, as the cutout size increases up to $s/W_b = 0.57$, the reduction in axial stiffness due to buckling varies between 44 and 35 percent. For the plate with $s/W_b = 0.86$, the reduction in axial stiffness is approximately 67 percent.

### Square Plates With Elliptical Cutouts

Experimental results were obtained for square plates with eight different elliptical cutout sizes. The ratio of elliptical cutout width to plate width for each panel is constant and is given by $2b/W_b = 0.6$. The ratio of cutout height to plate width $2a/W_b$ ranges from 0.05 to 0.7. The original motivation for examining this particular range of elliptical cutout sizes arose from previous studies of square plates with circular cutouts that indicated increases in buckling strain with increasing cutout size (e.g., see fig. 3). The cutout size, buckling load, prebuckling stiffness, and postbuckling stiffness of each plate are presented in table 6. The curves of nondimensional load $P/P^o_{cr}$ versus nondimensional end-shortening $\Delta/\Delta^o_{cr}$ are presented in figure 10 as a function of the ratio of cutout height to plate width $2a/W_b$. The analytical values of buckling load $P^o_{cr}$ and end-shortening $\Delta^o_{cr}$ used in figure 10 are the same as those used in figure 3 for the square plates with circular cutouts.

The results presented in table 6 and figure 10 indicate that the prebuckling stiffnesses of the plates generally decrease slowly with increasing cutout height (about 14-percent difference as $2a/W_b$ increases from 0.05 to 0.7). This trend is consistent with the fact that most of the in-plane stiffness of the plates is dictated by the amount of cross-sectional area at the net section of the plate. The maximum decrease in prebuckling stiffness, compared with the stiffness of the plate without a cutout given in table 1, is approximately 44 percent for the plate with $2a/W_b = 0.7$.

The results presented in table 6 also indicate that the buckling loads of the plates generally decrease with increasing cutout size, except for the plate with $2a/W_b = 0.3$. A comparison of the results for the plate with $d/W_b = 0$ in table 1 with the results

in table 6 indicates that the plates with $2a/W_b$ = 0.05, 0.1, and 0.2 buckle at loads approximately 38, 27, and 14 percent higher than the corresponding square plate without a cutout, respectively. Moreover, these values are conservative comparisons, since the plates with the elliptical cutouts are, on the average, about 3.4 percent thinner than the corresponding plate without a cutout. A 3.4-percent increase in thickness corresponds to approximately an 11-percent increase in buckling load for a plate without a cutout. The moire-fringe data indicate that the plate with $2a/W_b = 0.3$ buckled into a mode shape that occupied the right half of the plate and then immediately exhibited a change in buckle pattern to the usual centrally located mode shape that consisted of one half-wave along the plate length and width. The presence of this unusual buckle pattern appears to be the result of a nonuniform load introduction into the plate that is associated with improper machining of the loaded edges.

Average buckling strains for the plates with $0.1 \leq 2a/W_b \leq 0.7$ obtained from the approximate analysis and the average buckling strains of the test specimens are shown in figure 11. The average buckling strains shown in this figure are defined by the ratio of buckling load to prebuckling stiffness $P_{cr}/EA$ and are plotted as a function of the ratio of cutout height to plate width $2a/W_b$. The analytical results are based on nominal plate dimensions and the average thickness previously presented. Accurate analytical results for the plate with $2a/W_b = 0.05$ were not obtained because of limitations of the approximate analysis. These analytical and experimental results indicate that the buckling strain is essentially constant for $0.1 \leq 2a/W_b \leq 0.7$, with the exceptions of the plate with $2a/W_b = 0.3$ that buckled into the unusual mode as previously mentioned and the plate with $2a/W_b = 0.05$. The plate with $2a/W_b = 0.05$ exhibited the largest buckling load of the plates with elliptical cutouts and exhibited a somewhat smaller prebuckling stiffness than the plates with $2a/W_b = 0.1$ and 0.2. These attributes account for the relatively large buckling strain of the plate with $2a/W_b = 0.05$ shown in figure 11. The generally small variation in buckling strain with cutout height suggests that there is not a great deal of scatter in the experimental data. The buckling mode shapes for all the plates, except the plate with $2a/W_b = 0.3$, consisted of one half-wave along both the plate length and width.

Results presented in table 6 and figure 10 also indicate that the initial postbuckling stiffnesses of the plates generally decrease with increasing cutout height. The largest decrease is exhibited by the plate with $2a/W_b = 0.7$ and approximately 45 percent of the stiffness of the corresponding plate without a cutout. The initial postbuckling stiffness varies by approximately 27 percent as the cutout height changes. Comparison of the prebuckling stiffness with the postbuckling stiffness given in table 6 for each specimen indicates that, as the cutout height increases, the reduction in axial stiffness due to buckling varies from 25 to 40 percent for the full range of cutout sizes.

### Overall Behavior Trends

The experimental results presented in this paper include a wide range of cutout sizes, three cutout shapes, and three plate aspect ratios. Typically, only one specimen was tested for each combination of cutout size, cutout shape, and plate aspect ratio. Because of the limited amount of testing on each specimen type, the actual degree of scatter in the experimental data is not well-known. The buckling strain data presented in this paper, however, does suggest that the scatter is not large. Thus, the experimental data presented in this paper are useful in identifying overall behavior trends exhibited by each family of plates studied.

Results showing a trend of generally increasing buckling load with increasing circular cutout size were reported for simply supported rectangular isotropic plates with plate aspect ratios of 1 and 2 in reference 7. The results presented in tables 1 through 5 and in figure 3 indicate a similar behavior trend for square plates with circular cutouts and for rectangular plates ($L/W$ = 3 and 5) with circular and square cutouts. Also, the results indicate that the plates with square cutouts buckle at approximately the same strains as the corresponding plates with circular cutouts. For the plates in the present study, the loaded edges are clamped, and the unloaded edges are simply supported.

To indicate the overall postbuckling behavior trends of square and rectangular plates, results of the change in initial postbuckling stiffness due to circular or square cutouts are presented in figure 12. Specifically, the results presented in this figure show stiffness changes as a function of the plate aspect ratio $L/W$ and the ratio of cutout width to plate width ($d/W_b$ and $s/W_b$ for plates with circular and square cutouts, respectively). The stiffness changes shown in this figure are with respect to the initial postbuckling stiffness of the corresponding plates without a cutout. More specifically, results for each group of plates with the same plate aspect ratio are compared with results for the plates of the same plate aspect ratio and without a cutout.

The results presented in figure 12 indicate that in all cases the initial postbuckling stiffness of a

plate generally decreases as cutout size increases. The results also show that the reduction in stiffness becomes substantially less pronounced as the plate aspect ratio increases. Moreover, differences in initial postbuckling stiffness due to differences in cutout shape become more pronounced as the cutout size increases, and is on the order of 10 percent. The results presented in tables 1 through 5 indicate that the change in axial stiffness that a plate experiences as a result of buckling ranges from 31 to 44 percent for the full range of plate aspect ratios and square and circular cutout sizes considered. The results in figures 4 through 7 also indicate that the rectangular plates with square cutouts generally exhibit smaller segments of the load versus end-shortening curve, in which the initial postbuckling branch is linear, than the plates with circular cutouts. Moreover, the results indicate that as the plate aspect ratio increases, the linear postbuckling segment of the curves tends to get longer. The square plates have a much larger ratio of plate width to plate thickness and do not exhibit as much material yielding as the rectangular plates.

Results showing the change in prebuckling stiffness and the change in the initial postbuckling stiffness due to changes in elliptical cutout height are presented in figure 13. The results presented in this figure show stiffness changes as a function of the ratio of cutout height to plate width $2a/W_b$. The stiffness changes shown in the figure are also with respect to the initial postbuckling stiffness of the corresponding plate without a cutout. The results shown in figures 11 and 13 indicate that the prebuckling and initial postbuckling stiffnesses generally decrease with increasing cutout size, and that the postbuckling stiffness is more sensitive than the prebuckling stiffness and the buckling strain to changes in elliptical cutout height. The results indicate that the plates with the smaller cutout heights have nearly the same prebuckling stiffness and buckling strain as the other plates and that the plates with the smaller cutout heights have the most initial postbuckling stiffness. This observation suggests that it may be possible to tailor cutout shape to retain a high degree of buckling resistance and have a substantial amount of initial postbuckling stiffness.

## Concluding Remarks

An experimental study of the buckling and postbuckling behavior of square and rectangular compression-loaded isotropic plates with centrally located cutouts has been presented. A wide range of cutout sizes, three different cutout shapes, and three plate aspect ratios have been investigated. Specifically, results have been presented for square and rectangular plates with aspect ratios of 3 and 5 and with circular or square cutouts. The ratios of cutout width to plate width ranged from 0 to 0.86. Results have also been presented for square plates with elliptical cutouts that have a ratio of cutout width to plate width of 0.60 and several cutout heights.

Experimental results have been presented that indicate that the square and rectangular plates tested exhibit trends of increasing buckling strain and decreasing initial postbuckling stiffness with increasing circular and square cutout size. The rectangular plates tested that have circular and square cutouts with the same ratios of cutout width to plate width $\leq 0.57$ buckle at approximately the same strain level and exhibit approximately the same initial postbuckling stiffness. The results presented for square plates with circular cutouts and rectangular plates with circular and square cutouts also indicate that the reduction in initial postbuckling stiffness, with respect to the postbuckling stiffnesses of the corresponding plates without cutouts, decreases as the plate aspect ratio increases. The results also indicate that the square and rectangular plates lose between 30 and 45 percent of their axial stiffness as a result of buckling.

Results have been presented in the paper that show changes in cutout size and shape can cause a change in buckle pattern. Results have also been presented that indicate that plates with very large ratios of cutout width to plate width buckle locally in the two ligaments of the plate adjacent to the cutout. In each of these cases, substantial nonlinear prebuckling deformations due to material yielding were present. Also, the results show that a plate with a very large ratio of cutout width to plate width can exhibit a change in local buckle pattern.

Other results have been presented that indicate that square plates with elliptical cutouts that have a large ratio of cutout width to plate width generally have a decrease in prebuckling and initial postbuckling stiffness as the cutout height increases. However, the plates buckle at nearly the same strain level in each case. The results also indicate that the postbuckling stiffness is more sensitive to changes in elliptical cutout height than the prebuckling stiffness and the buckling strain. An important finding of this experimental study is the indication that it may be possible to tailor cutout shape and plate aspect ratio to improve buckling resistance and initial postbuckling stiffness.

NASA Langley Research Center
Hampton, VA 23665-5225
August 1, 1990

## References


1. Nemeth, Michael Paul: Buckling Behavior of Orthotropic Composite Plates With Centrally Located Cutouts. Ph.D. Diss., Virginia Polytechnic Inst. & State Univ., May 1983.
2. Nemeth, Michael P.; Stein, Manuel; and Johnson, Eric R.: *An Approximate Buckling Analysis for Rectangular Orthotropic Plates With Centrally Located Cutouts.* NASA TP-2528, 1986.
3. Nemeth, Michael P.: Buckling Behavior of Compression-Loaded Symmetrically Laminated Angle-Ply Plates With Holes. *AIAA J.*, vol. 26, no. 3, Mar. 1988, pp. 330–336.
4. Yu, Wei-Wen; and Davis, Charles S.: Buckling Behavior and Post-Buckling Strength of Perforated Stiffened Compression Elements. *The First Specialty Conference on Cold Formed Steel Structures*, Wei-Wen Yu, ed., Civil Engineering Dept., Univ. of Missouri-Rolla 1971, pp. 58–64.
5. Martin, James: Buckling and Postbuckling of Laminated Composite Square Plates With Reinforced Central Circular Holes. Ph.D. Diss., Case Western Reserve Univ., 1972.
6. Yu, Wei-Wen; and Davis, Charles S.: Cold-Formed Steel Members With Perforated Elements. *J. Struct. Div.*, American Soc. Civ. Eng., vol. 99, no. ST10, Oct. 1973, pp. 2061–2077.
7. Ritchie, D.; and Rhodes, J.: Buckling and Post-Buckling Behavior of Plates With Holes. *Aeronaut. Q.*, vol. 26, pt. 4, Nov. 1975, pp. 281–296.
8. Starnes, James H., Jr.; and Rouse, Marshall: Postbuckling and Failure Characteristics of Selected Flat Rectangular Graphite-Epoxy Plates Loaded in Compression. *A Collection of Technical Papers — AIAA/ASME/ASCE/AHS 22nd Structures, Structural Dynamics & Materials Conference, Part 1*, Apr. 1981, pp. 423–434. (Available as AIAA-81-0543.)
9. Roberts, T. M.; and Azizian, Z. G.: Strength of Perforated Plates Subjected to In-Plane Loading. *Thin-Walled Structures*, vol. 2, no. 2, 1984, pp. 153–164.
10. Narayanan, R.; and Chow, R. Y.: Ultimate Capacity of Uniaxially Compressed Perforated Plates. *Thin-Walled Structures*, vol. 2, no. 3, 1984, pp. 241–264.
11. VandenBrink, Dennis J.; and Kamat, Manohar P.: Post-Buckling Response of Isotropic and Laminated Composite Square Plates With Circular Holes. *Fifth International Conference on Composite Materials*, W. C. Harrigan, Jr., J. Strife, and A. K. Dhingra, eds., Metallurgical Soc., Inc., c.1985, pp. 1393–1409.
12. Nemeth, Michael P.: *Buckling and Postbuckling Behavior of Square Compression-Loaded Graphite-Epoxy Plates With Circular Cutouts.* NASA TP-3007, 1989.
13. Nemeth, Michael P.: *A Buckling Analysis for Rectangular Orthotropic Plates With Centrally Located Cutouts.* NASA TM-86263, 1984.

Table 1. Experimental Buckling Loads, Prebuckling Stiffnesses, and Initial Postbuckling Stiffnesses for Square Plates With Circular Cutouts

[All plates buckled into one half-wave along the plate length and width unless otherwise noted]

| Specimen | Cutout diameter to plate width, $d/W_b$ | Buckling load, kN (lb) | Prebuckling stiffness, kN/cm (lb/in.) | Initial postbuckling stiffness, kN/cm (lb/in.) |
|---|---|---|---|---|
| A1 | 0 | 8.327 (1872) | 947.679 (541 139) | 576.519 (329 201) |
| A2 | .1 | 8.131 (1828) | 835.952 (477 341) | 541.305 (309 093) |
| A3 | .2 | 7.722 (1736) | 813.096 (464 290) | 527.971 (301 479) |
| A4 | .3 | 7.366 (1656) | 746.819 (426 445) | 486.353 (277 715) |
| A5 | .4 | 8.042 (1808) | 683.998 (390 573) | 428.777 (244 838) |
| A6 | .5 | [a]8.928 (2007) | 571.239 (326 186) | 358.590 (204 760) |
| A7 | .6 | 8.874 (1995) | 547.319 (312 527) | 330.788 (188 885) |

[a]Mode shape consisted of a slightly off-centered pattern.

Table 2. Experimental Buckling Loads, Prebuckling Stiffnesses, and Initial Postbuckling Stiffnesses for Rectangular Plates With Circular Cutouts

[$L/W = 3$ for all plates; all plates buckled into one half-wave across the plate width and three half-waves along the plate length unless otherwise noted]

| Specimen | Initial cutout diameter to plate width, $d/W_b$ | Buckling load, kN (lb) | Prebuckling stiffness, kN/cm (lb/in.) | Initial postbuckling stiffness, kN/cm (lb/in.) |
|---|---|---|---|---|
| B1 | 0 | 15.057 (3385) | 327.438 (186 972) | 203.086 (115 965) |
| B2 | 0 | 15.538 (3493) | 329.571 (188 190) | 198.949 (113 603) |
| B3 | .14 | 15.404 (3463) | 329.846 (188 347) | 198.869 (113 557) |
| B4 | .29 | 14.733 (3312) | 294.772 (168 319) | 204.159 (116 578) |
| B5 | .57 | 17.054 (3834) | 263.477 (150 449) | 163.379 ( 93 292) |
| B6 | .86 | [a]13.647 (3068) | 173.139 ( 98 865) | [b]43.295 ( 24 722) |
| | | [c]14.132 (3177) | | [b]31.341 ( 17 896) |

[a]Local buckling of plate ligament adjacent to cutout.
[b]Tangent stiffness at buckling.
[c]Second local buckling mode (see fig. 8).

Table 3. Experimental Buckling Loads, Prebuckling Stiffnesses, and Initial Postbuckling Stiffnesses for Rectangular Plates With Square Cutouts

[$L/W = 3$ for all plates; all plates buckled into one half-wave across the plate width and three half-waves along the plate length unless otherwise noted]

| Specimen | Cutout width to plate width, $s/W_b$ | Buckling load, kN (lb) | Prebuckling stiffness, kN/cm (lb/in.) | Initial postbuckling stiffness, kN/cm (lb/in.) |
|---|---|---|---|---|
| C1 | 0.14 | 15.093 (3393) | 331.412 (189 241) | 198.664 (113 440) |
| C2 | .29 | 14.519 (3264) | 301.861 (172 367) | 194.033 (110 796) |
| C3 | .57 | [a]18.425 (4142) | 250.216 (142 877) | 152.665 ( 87 174) |
| C4 | .86 | [b]13.896 (3124) | 147.346 ( 84 137) | [c]20.229 ( 11 551) |

[a]Mode shape consisted of four half-waves along plate length.
[b]Local buckling of plate ligament adjacent to cutout.
[c]Tangent stiffness at buckling.

Table 4. Experimental Buckling Loads, Prebuckling Stiffnesses, and Initial Postbuckling Stiffnesses for Rectangular Plates With Circular Cutouts

[$L/W = 5$ for all plates; all plates buckled into one half-wave across the plate width and five half-waves along the plate length unless otherwise noted]

| Specimen | Cutout diameter to plate width, $d/W_b$ | Buckling load, kN (lb) | Prebuckling stiffness, kN/cm (lb/in.) | Initial postbuckling stiffness, kN/cm (lb/in.) |
|---|---|---|---|---|
| D1 | 0 | 15.106 (3396) | 212.464 (121 320) | 118.634 (67 742) |
| D2 | 0 | 14.581 (3278) | 206.834 (118 105) | 117.368 (67 019) |
| D3 | .14 | 14.973 (3366) | 209.951 (119 885) | 118.545 (67 691) |
| D4 | .29 | 14.208 (3194) | 203.827 (116 388) | 121.839 (69 572) |
| D5 | .57 | 15.222 (3422) | 187.788 (107 230) | 111.680 (63 771) |
| D6 | .86 | 14.457 (3250) | 135.396 ( 77 313) | [a]31.038 (17 723) |

[a]Tangent stiffness at buckling.

Table 5. Experimental Buckling Loads, Prebuckling Stiffnesses, and Initial Postbuckling Stiffnesses for Rectangular Plates With Square Cutouts

[$L/W = 5$ for all plates; all plates buckled into one half-wave across the plate width and five half-waves along the plate length unless otherwise noted]

| Specimen | Cutout width to plate width, $s/W_b$ | Buckling load, kN (lb) | Prebuckling stiffness, kN/cm (lb/in.) | Initial postbuckling stiffness, kN/cm (lb/in.) |
|---|---|---|---|---|
| E1 | 0.14 | 15.146 (3405) | 214.791 (122 649) | 122.619 (70 017) |
| E2 | .29 | 14.893 (3348) | 205.863 (117 551) | 118.247 (67 521) |
| E3 | .57 | [a]16.276 (3659) | 180.494 (103 065) | 117.288 (66 973) |
| E4 | .86 | [b]13.260 (2981) | 118.948 ( 67 921) | [c]39.531 (22 573) |

[a]Mode shape consisted of six half-waves along plate length.
[b]Local buckling of plate ligament adjacent to cutout.
[c]Tangent stiffness at buckling.

Table 6. Experimental Buckling Loads, Prebuckling Stiffnesses, and Initial Postbuckling Stiffnesses for Square Plates With Elliptical Cutouts

[$2b/W_b = 0.6$ for all plates; all plates buckled into one half-wave along the plate length and width unless otherwise noted]

| Specimen | Cutout height to plate width, $2a/W_b$ | Buckling load, kN (lb) | Prebuckling stiffness, kN/cm (lb/in.) | Initial postbuckling stiffness, kN/cm (lb/in.) |
|---|---|---|---|---|
| F1 | 0.05 | 11.481 (2581) | 609.250 (347 891) | 455.589 (260 148) |
| F2 | .1 | 10.565 (2375) | 662.293 (378 179) | 470.377 (268 592) |
| F3 | .2 | 9.515 (2139) | 608.306 (347 352) | 457.988 (261 518) |
| F4 | .3 | [a]11.250 (2529) | 592.622 (338 396) | 383.741 (219 122) |
| F5 | .4 | 8.158 (1834) | 590.069 (336 938) | 377.724 (215 686) |
| F6 | .5 | 8.794 (1977) | 539.932 (308 309) | 352.567 (201 321) |
| A7 | .6 | 8.874 (1995) | 547.319 (312 527) | 330.788 (188 885) |
| F7 | .7 | 7.829 (1760) | 532.988 (304 344) | 316.610 (180 789) |

[a]Mode shape consisted of an off-centered pattern.

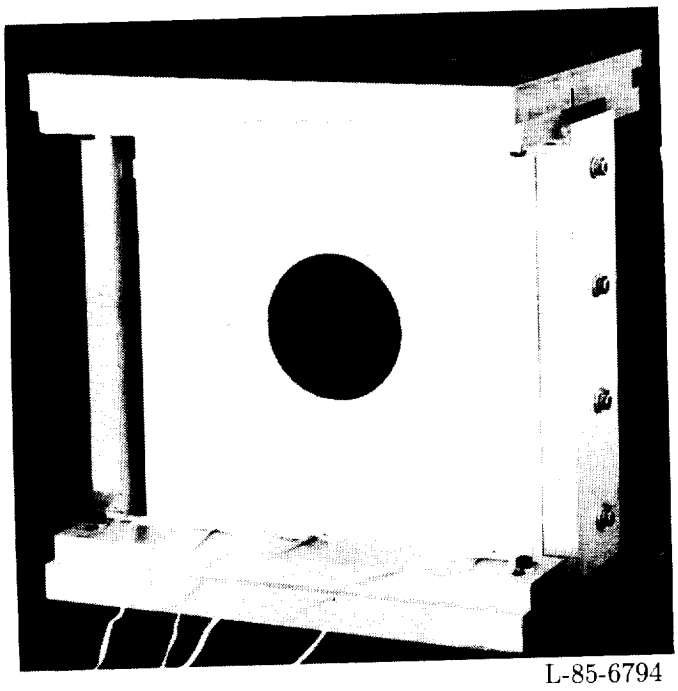


(a) Specimen mounted in test mixture.

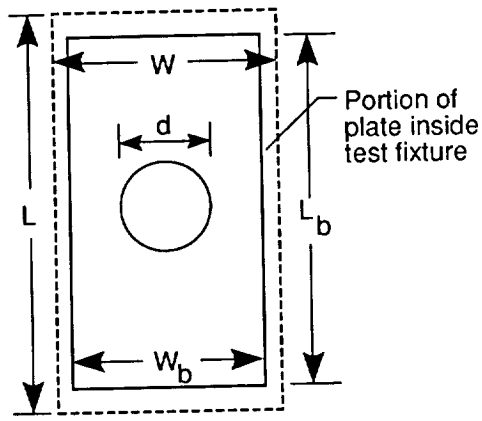


(b) Geometry of a plate with a circular cutout.

Figure 1. Test specimen and geometry when mounted in text fixture.

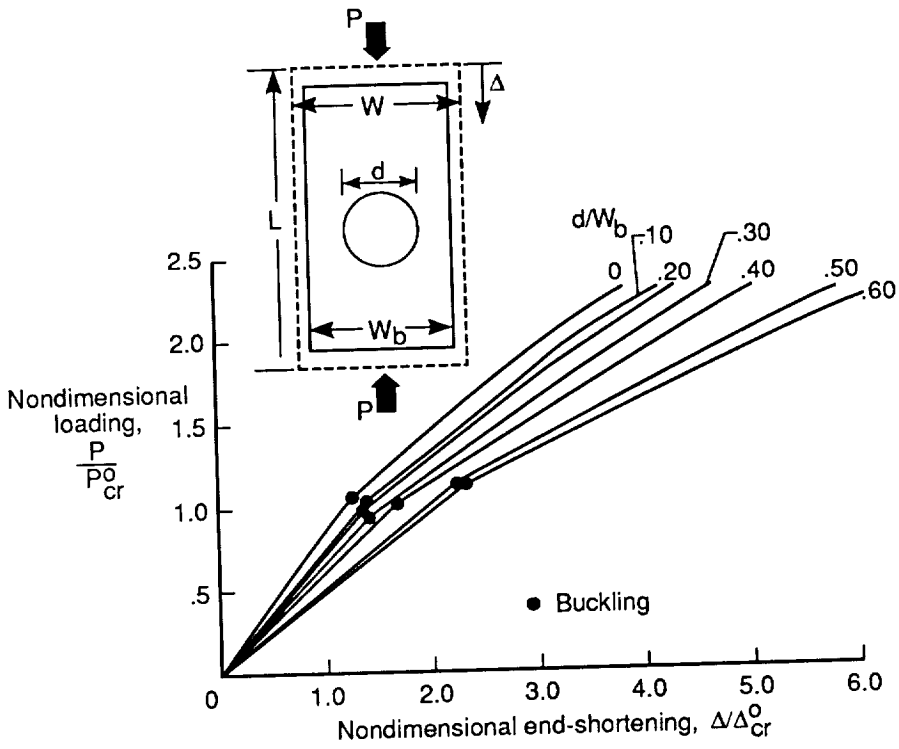


Figure 2. Nondimensional load versus end-shortening experimental results for square plates with central circular cutouts.

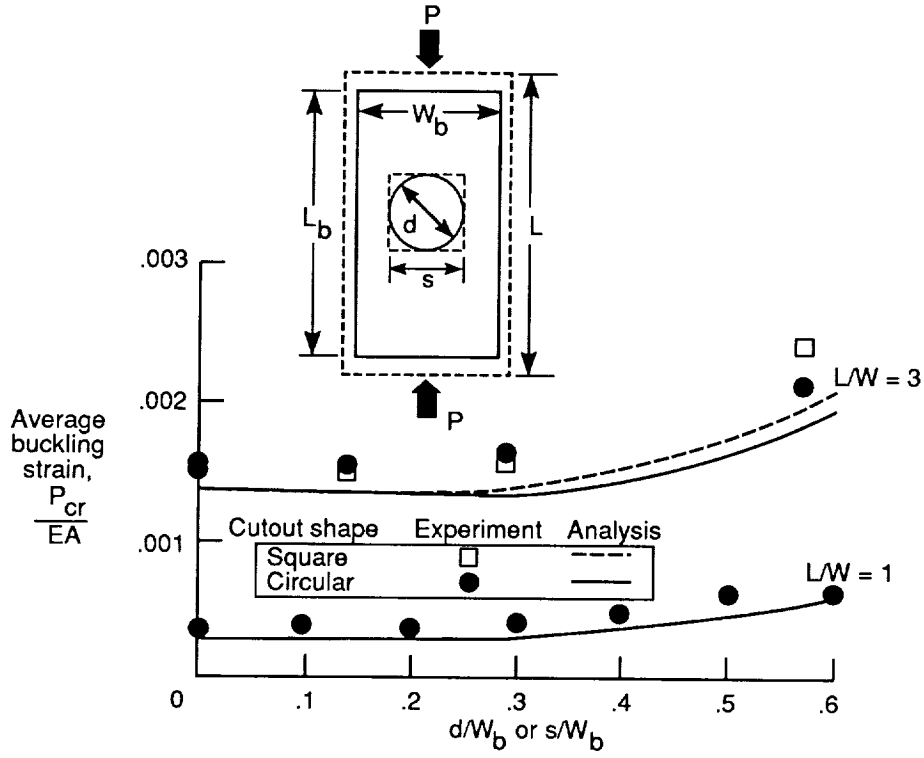


Figure 3. Average buckling strains for square and rectangular plates with circular and square cutouts.

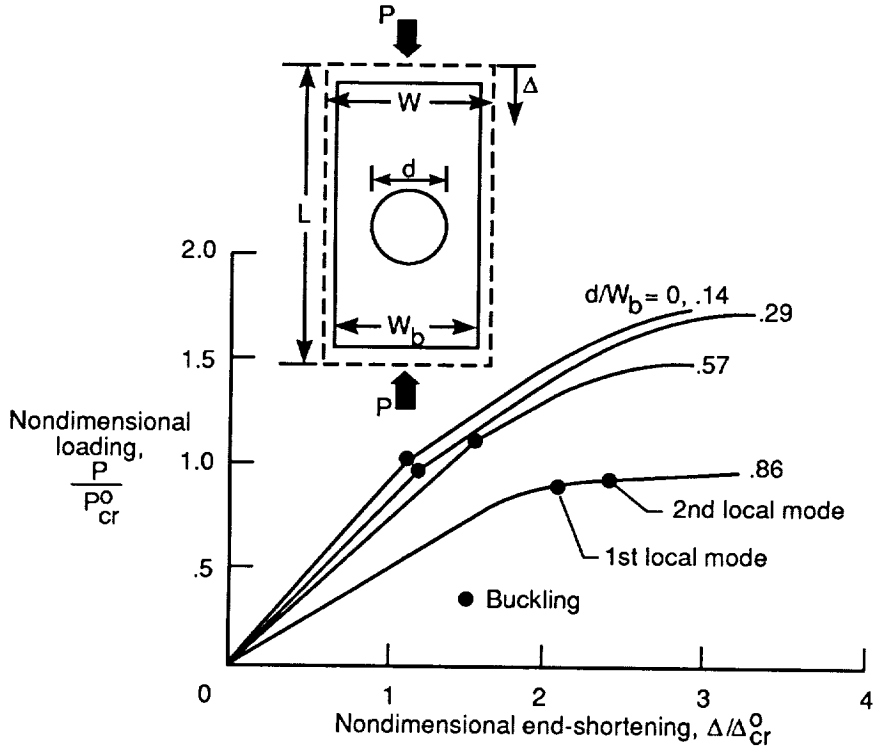


Figure 4. Nondimensional load versus end-shortening experimental results for rectangular plates with central circular cutouts and $L/W = 3$.

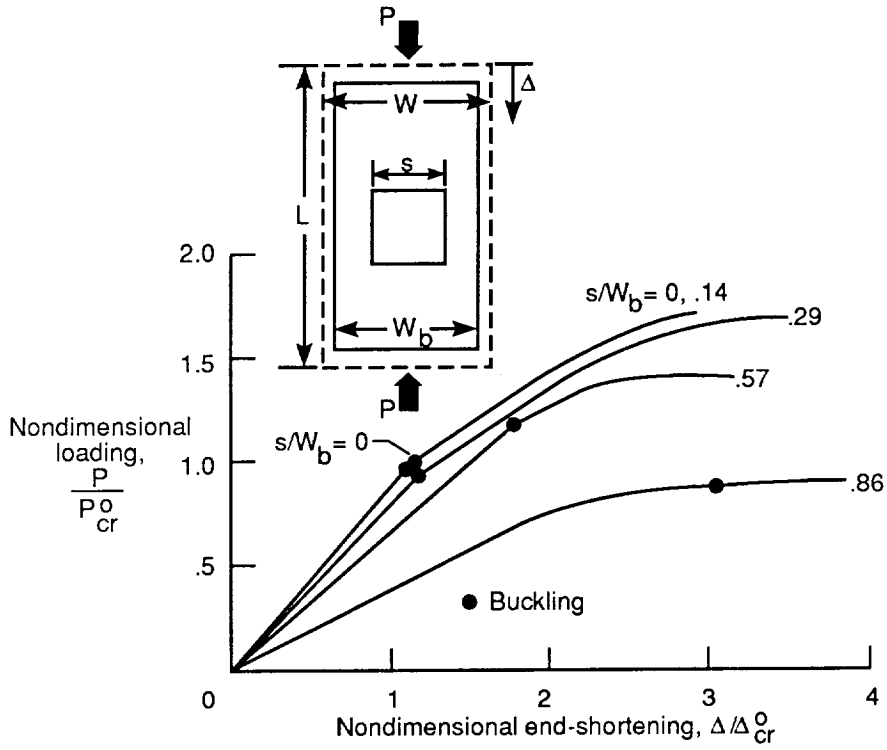


Figure 5. Nondimensional load versus end-shortening experimental results for rectangular plates with central square cutouts and $L/W = 3$.

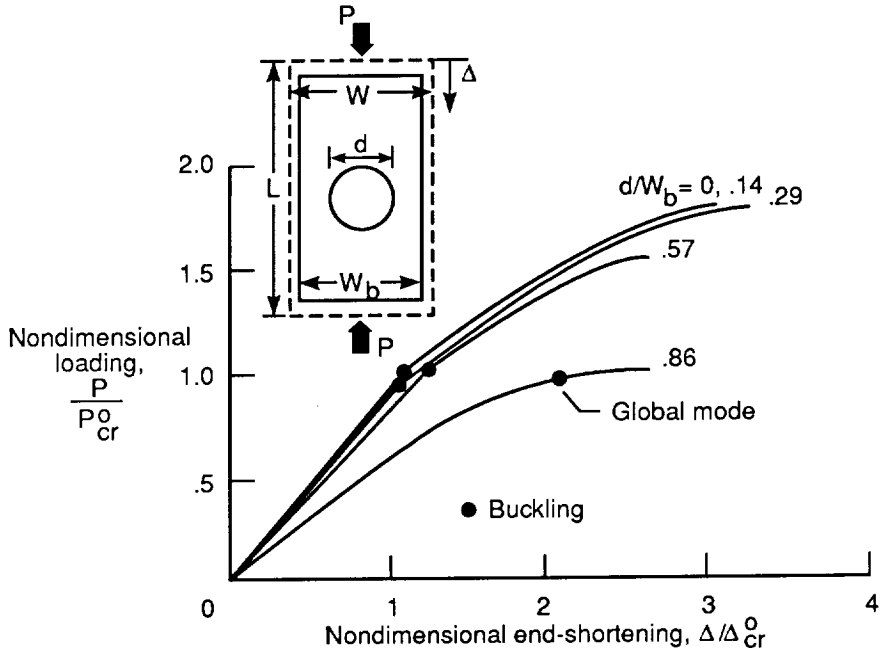


Figure 6. Nondimensional load versus end-shortening experimental results for rectangular plates with central circular cutouts and $L/W = 5$.

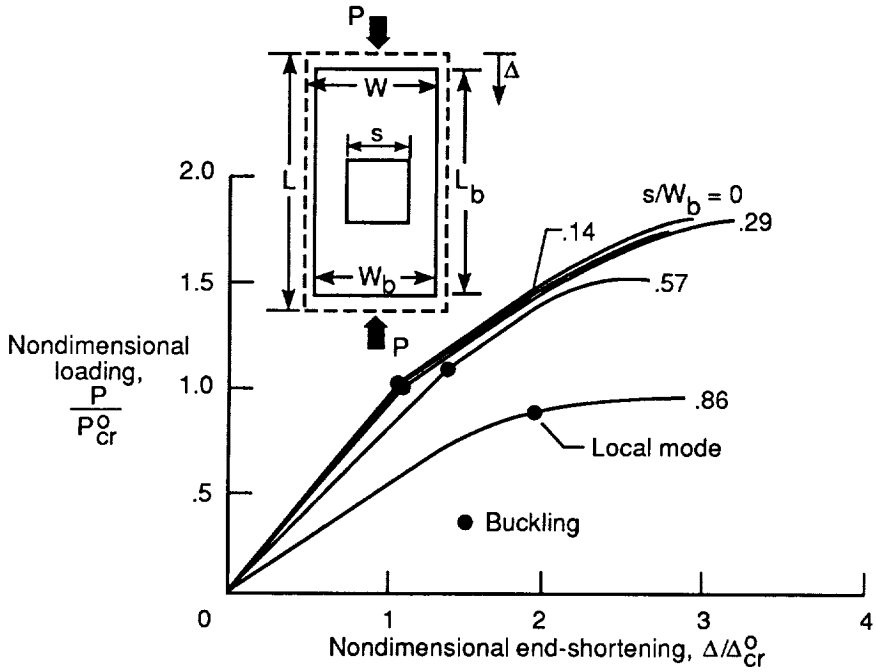


Figure 7. Nondimensional load versus end-shortening experimental results for rectangular plates with central square cutouts and $L/W = 5$.

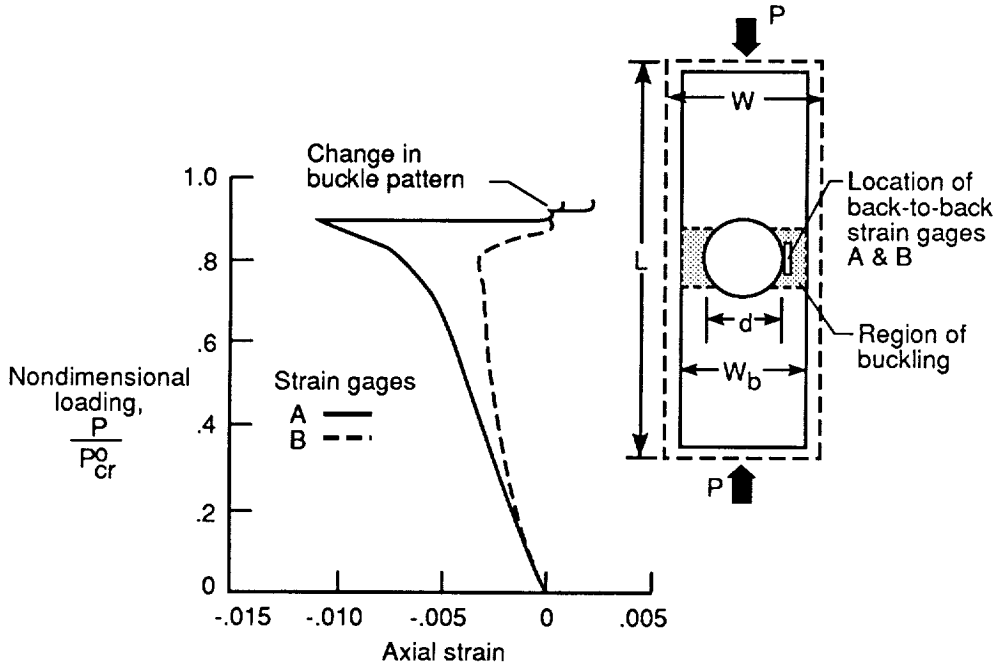


Figure 8. Strain near cutout in plate with $L/W = 3$ and $d/W_b = 0.86$.

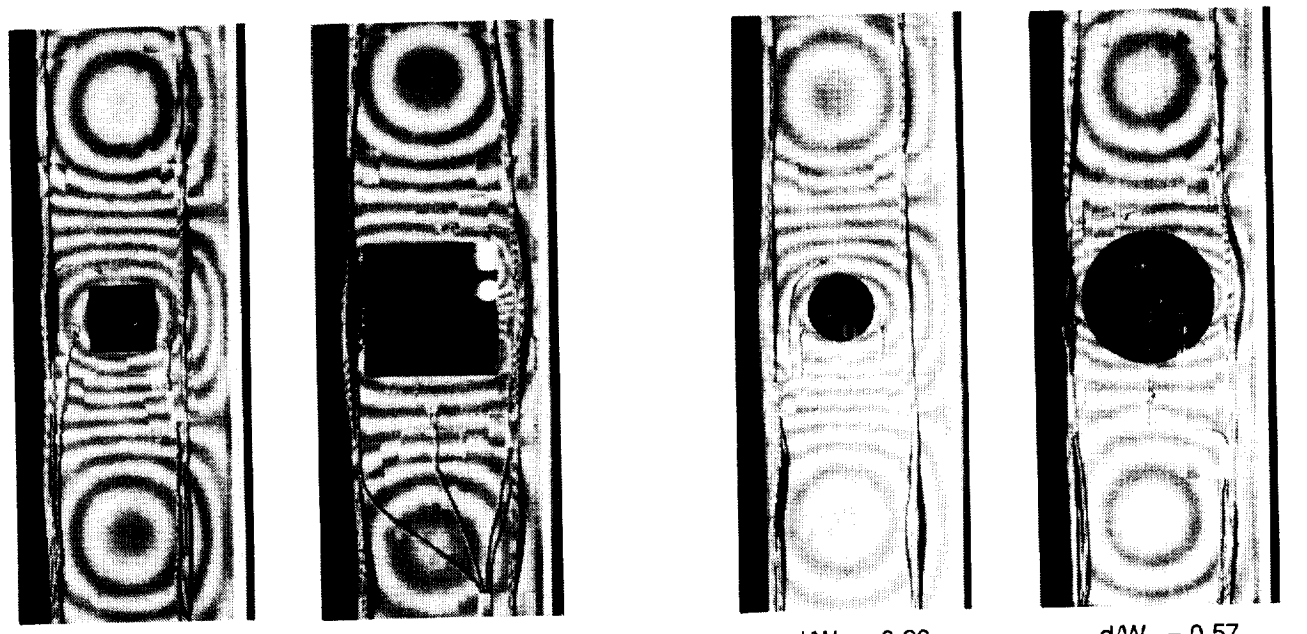


(a) Square cutouts.

(b) Circular cutouts.

Figure 9. Buckle patterns for plates with square and circular cutouts with $L/W = 3$.

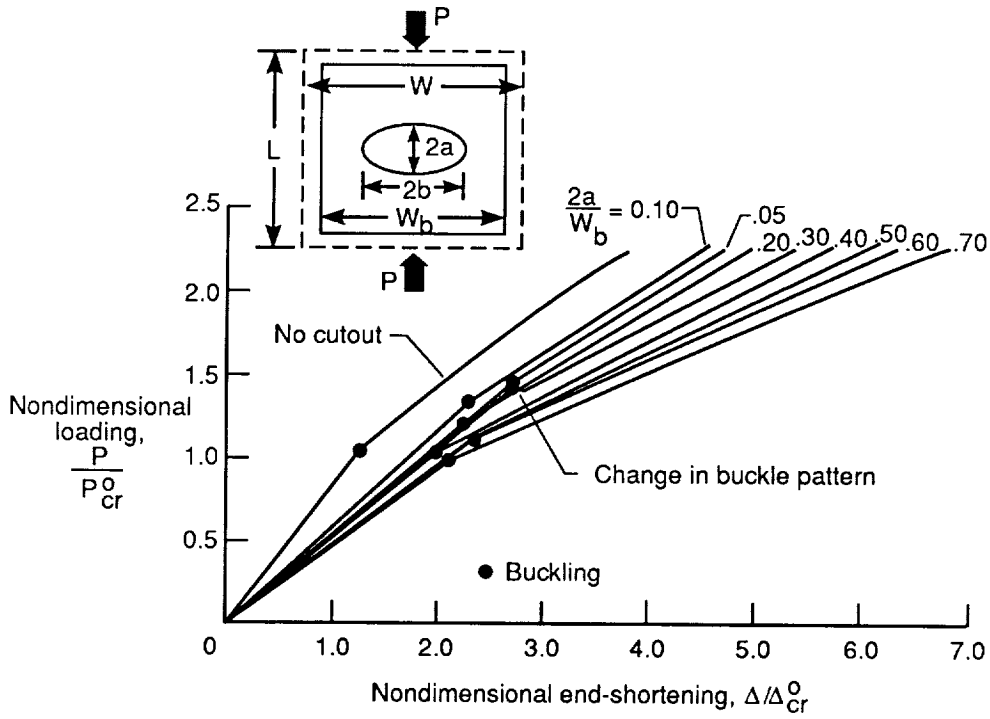


Figure 10. Nondimensional load versus end-shortening experimental results for square plates with central elliptical cutouts ($2b/W_b = 0.6$).

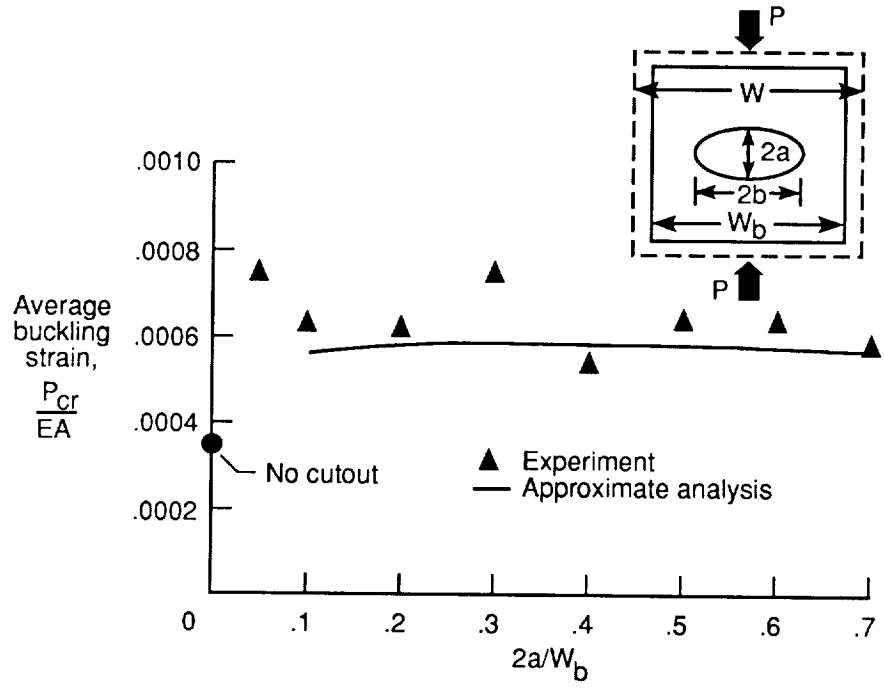


Figure 11. Average buckling strains for square plates with elliptical cutouts ($2b/W_b = 0.6$).

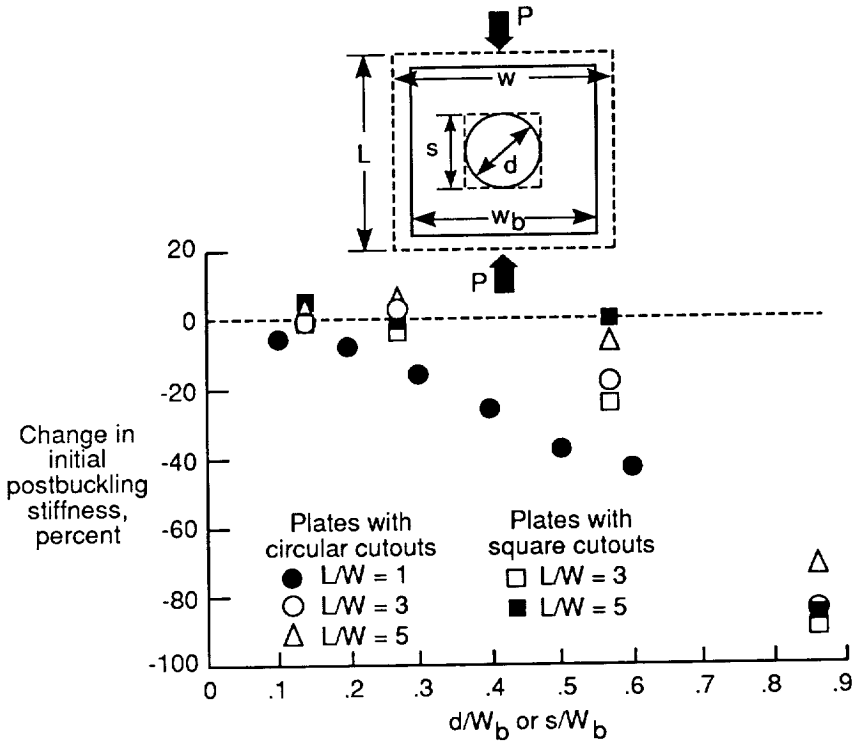


Figure 12. Change in initial postbuckling stiffness of square and rectangular plates with circular and square cutouts. (Change in stiffness is with respect to stiffness of corresponding plate without a cutout.)

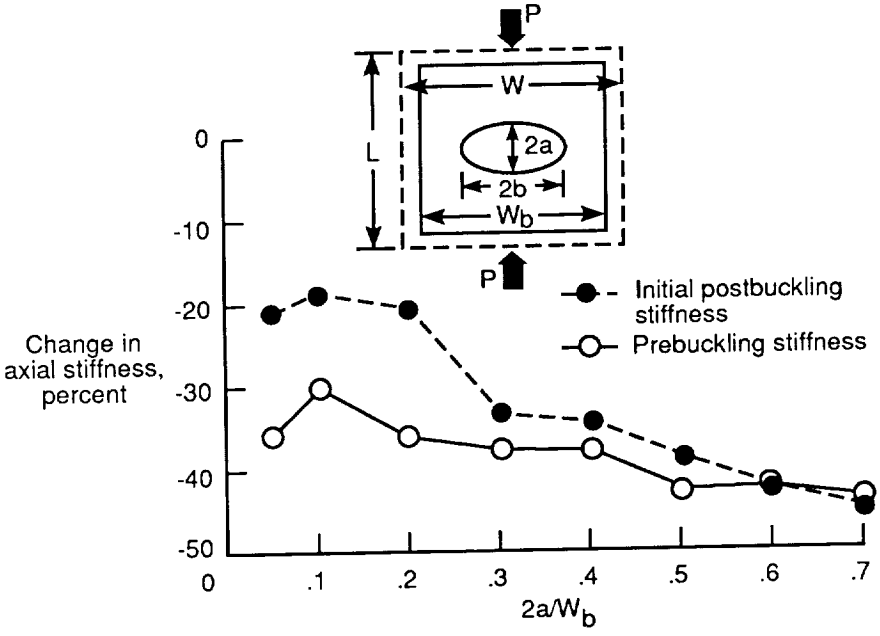


Figure 13. Change in prebuckling and initial postbuckling stiffness of square plates with elliptical cutouts. (Change in stiffness is with respect to stiffness of corresponding plate without a cutout.) All plates have $2b/W_b = 0.6$.

NASA
National Aeronautics and Space Administration

# Report Documentation Page

| 1. Report No. | 2. Government Accession No. | 3. Recipient's Catalog No. |
|---|---|---|
| NASA TP-3024 | | |

| 4. Title and Subtitle | 5. Report Date |
|---|---|
| Buckling and Postbuckling Behavior of Compression-Loaded Isotropic Plates With Cutouts | September 1990 |
| | 6. Performing Organization Code |
| 7. Author(s) | 8. Performing Organization Report No. |
| Michael P. Nemeth | L-16789 |
| 9. Performing Organization Name and Address | 10. Work Unit No. |
| NASA Langley Research Center<br>Hampton, VA 23665-5225 | 505-63-01-08 |
| | 11. Contract or Grant No. |
| 12. Sponsoring Agency Name and Address | 13. Type of Report and Period Covered |
| National Aeronautics and Space Administration<br>Washington, DC 20546-0001 | Technical Paper |
| | 14. Sponsoring Agency Code |

15. Supplementary Notes

Presented at the 31st AIAA/ASME/ASCE/AHS Structures, Structural Dynamics, and Materials Conference, Long Beach, California, April 2 4, 1990.

16. Abstract

An experimental study of the buckling and postbuckling behavior of square and rectangular compression-loaded aluminum plates with centrally located circular, square, and elliptical cutouts is presented. Experimental results indicate that the plates exhibit overall trends of increasing buckling strain and decreasing initial postbuckling stiffness with increasing cutout width. Corresponding plates with circular and square cutouts of the same width buckle at approximately the same strain level and exhibit approximately the same initial postbuckling stiffness. Results show that the reduction in initial postbuckling stiffness due to a cutout generally decreases as the plate aspect ratio increases. Other results presented in this paper indicate that square plates with elliptical cutouts and a large ratio of cutout width to plate width generally lose prebuckling and initial postbuckling stiffness as the cutout height increases. However, the plates buckle at essentially the same strain level. Results also indicate that postbuckling stiffness is more sensitive to changes in elliptical cutout height than are prebuckling stiffness and buckling strain.

| 17. Key Words (Suggested by Authors(s)) | 18. Distribution Statement |
|---|---|
| Buckling<br>Postbuckling<br>Prebuckling stiffness<br>Buckling strain | Unclassified Unlimited<br><br>Subject Category 39 |

| 19. Security Classif. (of this report) | 20. Security Classif. (of this page) | 21. No. of Pages | 22. Price |
|---|---|---|---|
| Unclassified | Unclassified | 20 | A03 |





For sale by the National Technical Information Service, Springfield, Virginia 22161-2171

National Aeronautics and
Space Administration
Code NTT-4

Washington, D.C.
20546-0001





NASA